STANDARD MODEL ELECTROWEAK MEASUREMENTS AT LEP

FRANCESCO SPANÒ
CERN, European Center for Nuclear Research
1211 Genève 23 - Switzerland
francesco.spano@cern.ch

The current status of electroweak physics results from LEP is reviewed. Particular emphasis is placed on the latest results on the properties of the Z and W bosons. The updated status of the global electroweak fit to the standard model and the resulting standard model Higgs mass limits are presented.

1 Introduction

Electron-positron collision allow a detailed investigation of the standard model (SM) thanks to their clean experimental conditions.

The Large Electron-Positron collider (LEP) was operated at CERN for about 12 years (1989 - 2000) at increasing center of mass energies ($\sqrt{s}$): both at the Z^0 pole ($\sqrt{s} \approx 91$ GeV) and beyond ($\sqrt{s}$ = 160-209 GeV). Its maximum instantaneous luminosity was 0.5-1 10^{32} cm^{-2} s^{-1} with a 45 kHz bunch-crossing rate.

The four LEP multi-purpose detectors (ALEPH, DELPHI, L3, OPAL) collected an integrated luminosity of about 1000 pb^{-1} each (with about 700 pb^{-1} beyond the Z^0 pole). These data correspond to about 4.5 million Z^0 and about 11000 W pair events per experiment.

2 Z^0 physics

The Z^0 boson couples to fermion-anti-fermion pairs. A gauge-invariant description embeds its production in the two-fermion production process $e^+e^- \to f\bar{f}$.

They complement cross sections information to obtain the absolute size of the parity-violating couplings. In addition they allow universality tests by comparing $\sin\theta^f_{eff}$ and the ρ_f parameter ($\rho_f = M_W/(M_Z \cos^2\theta^f_{eff})$ i.e. the ratio of neutral and charged current interaction strengths).

2.1 Physics at the Z^0 resonance

The LEP Z^0 pole results are final[1].

• The two-fermion production cross section as a function of $\sqrt{s}$ yields both the Z^0 mass, M_Z and its total width, Γ_Z. The ratios of cross sections for different two-fermion processes provide the Z^0 partial widths and information about the relative strength of the Z^0 couplings to different final state fermions (see sections 1.4 and 1.5.1 of [1]).

The Z^0 lineshape parameters are known at the sub-per mil level as shown in table 1. A lineshape example is shown in Figure 1 (left).

M_Z	91.1875 ± 0.0021 GeV	σ^0_{had}	41.540 ± 0.037 nb
Γ_Z	2.4952 ± 0.0023 GeV	ρ_l	1.0050 ± 0.0010

Table 1: Z^0 lineshape basic parameters (from top to bottom): the Z^0 mass and width, the hadronic cross section at the pole and the ratio of neutral to charged current interaction strength for leptonic final states at the pole. The extracted values have non zero correlation matrix.

A fundamental by-product [1] is the determination of the number of light neutrino families, $N_\nu = 2.9840 \pm 0.0082$, by comparing the Z^0 invisible branching fraction measured at the pole ($(\Gamma_{inv}/\Gamma_{ll})^0 = 5.943 \pm 0.016$) with the expectation obtained from the standard model Z^0 decay into neutrinos ($(\Gamma_{\nu\nu}/\Gamma_{ll})^{SM} = 1.99125 \pm 0.00083$).

• The right and left-handed coupling of the Z^0 to fermions are different (see section 1.4 in [1]) and consequently violate parity invariance. In e^+e^- collisions Z^0 bosons can then be expected to exhibit a net polarization along the axis of colliding beams, even when the incoming particles are not polarized. The decay of polarized Z^0's results in fermions with net helicity and with asymmetric angular distributions with respect to the beam direction.

The effective electroweak mixing angle for leptons, $\sin\theta^{lept}_{eff}$ is obtained at LEP by measuring forward-backward asymmetries at the Z^0 pole for different final state fermions and using the corresponding left-right forward-backward asymmetries measured at SLD to account for quark or electron couplings (see section 1.5.3 of [1]). Three measurements are derived from leptonic final states only: asymmetry from Z^0 decay to leptons at the pole at LEP is complemented by τ polarization P^0_τ and left-right asymmetry A_l at the SLD. Quark final states at LEP provide three complementary results using forward-backward asymmetries for b and c quarks final states at the pole, (A^{0b}_{fb}, A^{0c}_{fb}) and the jet charge asymmetry. This is all summarized in Figure 1 (right). The combined result is $\sin\theta^{lept}_{eff} = 0.23153 \pm 0.00016$. A_l and A^{0b}_{fb} show a 3.2 σ discrepancy: this is the main contributor to the 3.7% least squared probability for the combined result. The systematic uncertainties in both measurements are considered to be under control (QCD and flavour corrections for A^{0b}_{fb}, beam polarization for A_l) and the discrepancy is treated as a fluctuation [1] rather than a sign of new physics.

2.2 Two fermion physics above the Z^0 resonance

The cross sections and asymmetries in two fermion events are also measured at higher $\sqrt{s}$ than the Z^0 pole ($\sqrt{s}$= 130 - 209 GeV). They test the standard model in a different physics regime: the pure Z^0 cross section decreases as the size of photon exchange and Z^0/γ interference become important and the total cross section falls off. Measurements are performed both for inclusive and for high-energy non-radiative events [a]. The LEP averages show good agreement with the standard model predictions and help put limits on new physics that could lead to visible effects in the selected final states at these energies, for example from contact interactions or Z' bosons [3].

Two of the most recent results are:

• OPAL final measurement of R_b [4] (ratio of the $b\bar{b}$ cross section to the $q\bar{q}$ cross section in e^+e^-collisions). R_b values (in figure 2 (left)) are compatible with SM expectations. The mean ratio of eight R_b measurements to their SM expectation is 1.055 ± 0.048.

[a] In addition to non-radiative events the inclusive sample consists of a sizeable fraction of radiative returns to the Z^0 peak via initial state radiation [2].

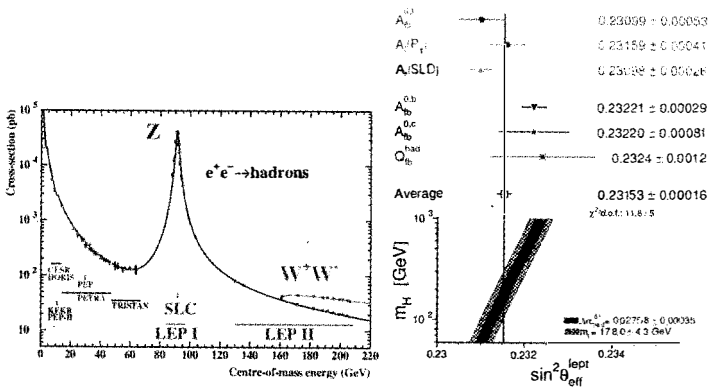

Figure 1: Left plot: Z^0 hadronic cross section; points are measurements and the solid line is the SM prediction. Various e^+e^- collider energy ranges are reported. Right plot: Comparison of the effective electroweak mixing angle $\sin\theta^{lept}_{eff}$ for leptons obtained from asymmetries depending on lepton couplings (top) only and also on quark couplings (bottom). The SM prediction is shown as a function of the Higgs mass. Vacuum polarization corrections and top mass uncertainty dominate the SM prediction uncertainty.

• L3 final result [5] on hadron and lepton pairs cross sections and lepton pairs asymmetries using both inclusive and non radiative sample. An overall good agreement is found with the standard model. An example is shown in figure 2 (right) for hadron cross section.

3 W physics at LEP

W bosons are pair-produced at LEP. The tree-level description of $e^+e^- \rightarrow W^+W^-$ is the so-called CC03 diagrams [2]. As each unstable W boson decays into lepton or quark pairs, a four fermion (4f) final state is obtained with three possible topologies. The fully leptonic channel $\ell\nu_\ell\ell\nu_\ell$ is characterized by two high energy isolated acoplanar leptons with large missing energy. The semi-leptonic channel $qq\ell\nu_\ell$ exhibits an isolated high energy lepton with two jets and missing energy. The qqqq channel features at least four jets and very little missing energy. The three branching ratios are about 10%, 46% and 44% respectively. Width effects and interfering $e^+e^- \rightarrow$ 4f diagrams destroy CC03 gauge invariance. CC03 diagrams are embedded in an $e^+e^- \rightarrow$ 4f description [6] with $O(\alpha)$ electroweak corrections that maintains gauge invariance and keeps theoretical uncertainties under control. This takes into account background from non-WW $e^+e^- \rightarrow$ 4f processes. The other significant background is represented by $e^+e^- \rightarrow Z^0/\gamma \rightarrow$ hadrons.

3.1 W pair production

W pair production (CC03 cross section) in the kinematic region explored by LEP shows a good consistency with the SM expectations incorporating $O(\alpha)$ electroweak corrections (only the W $\rightarrow \tau\nu_\tau$branching ratio is $\approx 2.8\ \sigma$ above its expectation). Final results for the W^+W^- cross sections and W branching rations are available from ALEPH, L3 and DELPHI. OPAL has preliminary results for $\sqrt{s}$ = 161- 189 GeV and final for $\sqrt{s}$ = 192 - 207 GeV. Good agreement with the SM prediction is also found for Z^0 pair production (main 4f background to W^+W^- after event selection). The results [3] are shown in Figure 3. The typical cross section for W^+W^- production beyond 180 GeV is about 17 pb.

3.2 W mass and width extraction

At threshold for W^+W^- production ($\sqrt{s} \approx 161$ GeV), the W mass is derived from the cross section measurement. Above threshold, real W bosons are reconstructed from their decay products

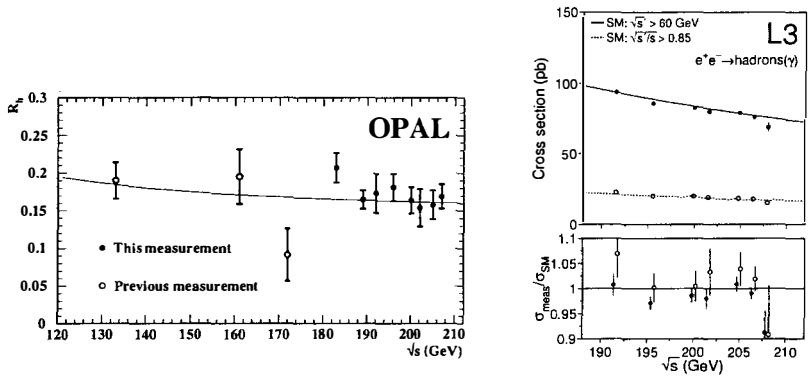

Figure 2: Left plot: R_b measurements from OPAL (points with error bars) compared to the SM prediction (solid line). Right plots: cross section for hadrons(γ) from L3 for the inclusive sample (filled symbols) and for the high energy sample (open symbols) compared to the SM predictions in solid (inclusive) and dashed (high-energy) lines (upper plot); ratios of measured cross sections to SM predictions (lower plot)

and mass and width extracted from appropriate event distributions.

Complex multi-step selections combining cut-based algorithms, likelihood discriminants and neural networks are used to separate signal from background. Typical efficiencies are around 80% for qq$\ell\nu_\ell$ and qqqq channels and 70% for $\ell\nu_\ell\ell\nu_\ell$ channel. Typical purities are 85% (qq$\ell\nu_\ell$), 80% (qqqq) and 90% ($\ell\nu_\ell\ell\nu_\ell$).

Above threshold $\ell\nu_\ell\ell\nu_\ell$ events are not reconstructed due to the two neutrinos in the final state and separate analyses[3] are carried out. To reconstruct the events, lepton identification in qq$\ell\nu_\ell$ channel is carried out; the event remnant is forced into two jet. Four jets are produced from qqqq events. DELPHI, L3 and OPAL allow for an additional gluon jet. Event-by-event kinematic fit use knowledge of the precise beam energy to constrain the total four-momentum. The event-by-event mass resolution is greatly improved. Various algorithms reduce jets-to-W mis-pairing in the qqqq channel: consistency with W decay kinematics (ALEPH, OPAL), multivariate selections and cuts in kinematic fit probability (OPAL and L3), combined information from all pairings (DELPHI, OPAL). The resulting jet-to-W pairing efficiency is 70%-90%.

Reconstructed distributions are compared with the expectation by a maximum likelihood technique to extract W mass and width. Three different methods are used to estimate the expected data distributions as a function of M_W and Γ_W. An analytic asymmetric **Breit-Wigner** function (OPAL) provides a robust and simple method for preliminary estimation. The analytic **convolution** of a modified Breit-Wigner [b] with an event-dependent detector response aims at using maximum information to reduce statistical uncertainty (DELPHI, OPAL). Both analytic methods need Monte Carlo (MC) calibration to correct biases. A **re-weighting** technique (ALEPH, L3, OPAL) generates expected data at arbitrary M_W and Γ_W using a single fully simulated MC sample. This fully exploits the knowledge encoded in the Monte-Carlo and minimizes possible bias effects.

3.3 W mass uncertainties

The LEP combined uncertainties on W mass as of Winter 2006[3] are illustrated in Table 2. The results are final for ALEPH[7], L3[8] and OPAL[9]. DELPHI results are still preliminary.

The main updates are as follows:

[b] To take into account initial state radiation and phase space effects.

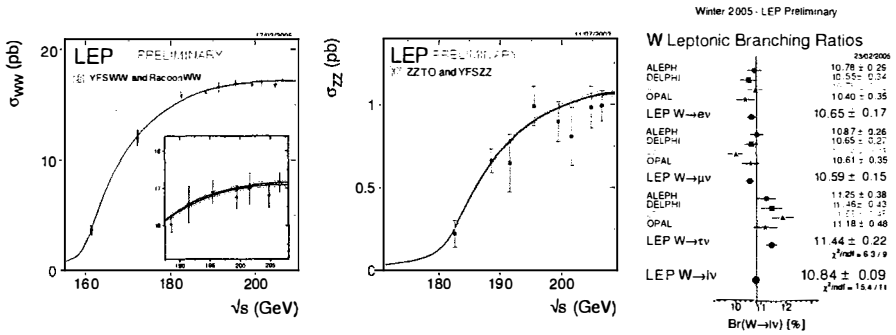

Figure 3: LEP combined results on W production and decay. Cross section measurement for W (left) and Z (center) pair production. W leptonic branching ratios are also shown (right).

Table 2: W mass uncertainties as of Winter 2006.

Source	Uncertainties on M_W(MeV)		
	$qq\ell\nu_\ell$	qqqq	Combined
QED (ISR/FSR,etc)	9	5	8
Hadronisation	14	20	15
Detector Systematics	11	8	10
LEP beam energy	9	9	9
Colour reconnection	-	31	7
Bose-Einstein Correlation	-	13	3
Other	3	11	4
Total Systematic	22	43	24
Statistical	31	43	26
Overall	38	61	35

LEP beam energy The final LEP energy calibration[10] helps decrease the associated uncertainty on M_W.

Bose-Einstein Correlation (BEC) Unaccounted quantum interference of identical bosons during hadronisation can correlate pions from different W bosons (inter-W BEC) and bias the M_W and Γ_W measurements. The uncertainties are set using the LUBOEI [11] model taking the difference between the presence and the absence of such correlations. Current studies at LEP show no evidence of inter-W correlations *à la* LUBOEI and the 'percentage' of LUBOEI Inter-W correlation present in data is shown to be linear in M_W uncertainty[3]. This is used, for each experiment, to achieve a data-driven reduction of M_W uncertainty (by 30%) used for the combined result.

Colour Reconnection (CR) Non-simulated colour cross-talk between decay products of different W bosons in qqqq channel can bias the M_W and Γ_W determination. Different models predict mass biases up to 200 MeV. The largest bias is foreseen by the SK model[12] with variable CR strength k. LEP experiments use a 'particle flow' technique[3] to establish a 68% C.L. limit on k. This provides a data-driven uncertainty on M_W and Γ_W. The major improvement is obtained by using estimates of jet angles which have low sensitivity CR effects: cutting out low momentum particles, reconstructing jets with cones of variable size, weighting momenta with a power of their magnitude. All final result use a momentum cut technique: with respect to

previous measurements, a 15% to 35% increase in M_W statistical uncertainty and a 30%-100% increase in M_W hadronization uncertainty are more than compensated by a two to three-fold reduction in M_W CR uncertainty.

The combined qqqq M_W uncertainty improves by without biasing the W mass result. The qqqq channel reaches a 23% weight in the combineation (up from 9% before BEC and CR reductions)[c].

Other uncertainties incorporate ignorance on photon radiation in $e^+e^- \to$ 4f, MC statistics and experiment-specific effects.

3.4 LEP and global combined results for W mass: status and outlook

The latest combined results[3] for W mass and width (Winter 2006) are shown in Figure 4.

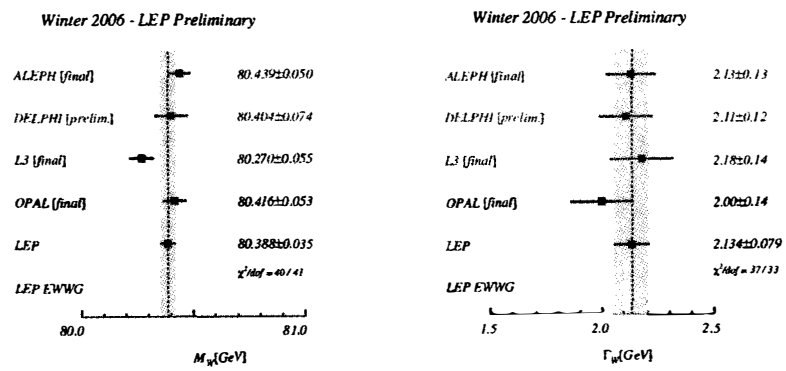

Figure 4: LEP W mass and width measurement as of Winter 2006

The theoretical prediction for M_W derived from the SM and the electroweak measurements is in good agreement with the measured LEP value. Results from W^+W^- threshold are included in the LEP combination. The updated LEP results are $M_W = 80.388 \pm 0.035$ GeV and $\Gamma_W = 2.134 \pm 0.079$ GeV.

The direct measurement of the W mass at LEP and at $p\bar{p}$ colliders (CERN SppS, Tevatron) are in very good agreement. The indirect results do not show any significant discrepancy with the possible exception of the NuTeV value. SM predictions based on the W mass and Top quark mass prefer a 'low' (below $\approx$ 219 GeV) SM Higgs mass value. The updated results[13] are summarized in Figure 5.

The final LEP result for W mass and width will profit from the final DELPHI result and will use combined LEP results on final state interaction parameters for a coherent reduction of the uncertainties. A reasonable target for the final LEP W mass uncertainty is an improvement of 1 or 2 MeV on the present value.

4 Standard model status: global fit and the Higgs

A global least-squared fit is performed to extract five SM parameters from which all the other oservables depend. The SM consistency requires that all the observables are determined as a function of the same free parameter values. The chosen parameters are: the QED and QCD coupling constants at the Z pole, $\alpha_{QED}(M_Z)$, $\alpha_{QCD}(M_Z)$, the masses of the Higgs boson, the

[c] M_W statistical uncertainty without including final state interactions effects would be 21 MeV, the current 26 MeV value shows that most of qqqq statistical power is being used.

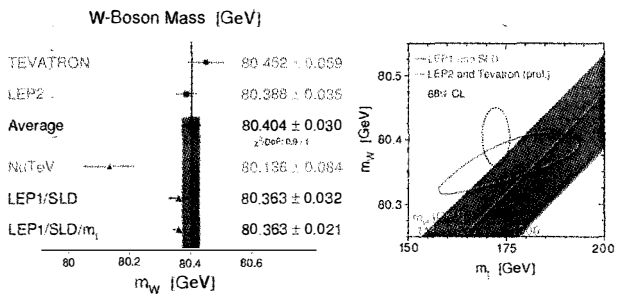

Figure 5: Direct and indirect W mass measurements (left) and SM consistency plot (right)

top quark and the Z boson. Eighteen observables measured in high momentum transfer events ($Q^2 \approx M_Z^2$) are used in the fit. The result is shown in Figure 6(left). The fit χ^2/d.o.f is 17.5/13 (probability($\chi^2 > \chi^2_{min}$) = 18%). The largest contribution to the fit χ^2 derives from A_{fb}^{0b} (about 2.8 σ) A_{fb}^{0b} favours high values of the Higgs mass, in contrast with M_W and the leptonic asymmetries. The high Q^2 parameters are used to derive predictions for low momentum transfer observables ($Q^2 \ll M_Z^2$). Good agreement is observed for parity violation in atoms and in Moeller scattering. The combination of left-handed effective coupling constants $g_{\nu Lud}$ derived from neutrino-nucleon scattering events in the NuteV experiment shows a discrepancy of about 2.8 σ with respect to its SM expectation. A sizeable theoretical effort is ongoing on uncertainties of radiative corrections and QCD effects affecting the measurement (see sec. 8.3.3 of [1]).

The resulting limits on the standard model Higgs mass [3] derived from the high Q^2 fit are shown in Figure 6 (right). At 95% confidence level, M_H is below 186 GeV (> 114.4 GeV from LEP direct searches). If LEP lower limit is included by renormalizing the probablity above it, the upper limit is 219 GeV. The limits show little sensitivity to the inclusion of low Q^2 data as the shift in the prediction is comparable with the theoretical uncertainty.

5 Conclusions

Z^0 physics, in the two fermion final state is understood at an impressive level. The final results from LEP determine the Z^0 lineshape parameters determined at the sub-per mil level. Two fermion physics and W pair production and decay are well understood above the Z^0 pole. The measurement of the mass and the width of the W boson is final for three experiments out of four. The best direct W mass measurement is achieved at LEP (Mw = 80.388 ± 0.035 GeV) with a 0.4 per mil relative uncertainty.

The general SM picture shows good global consistency pointing at an expected Higgs mass below 219 GeV. The standing discrepancies (A_{fb}^{0b}, $W \rightarrow \overline{\nu}_\tau$ branching ratio and NuTeV) show the need for new data and additional theoretical effort. LEP confirms its extremely successful record in thoroughly testing the standard model by the coherent combination of results from its four experiments.

Acknowledgments

The author would like to acknowledge the support of the European Union grant for young scientists. Richard Kellogg, Martin Grünewald, Luca Malgeri, Arno Straessner and Pat Ward are to be thanked for enlightening conversations and comments.

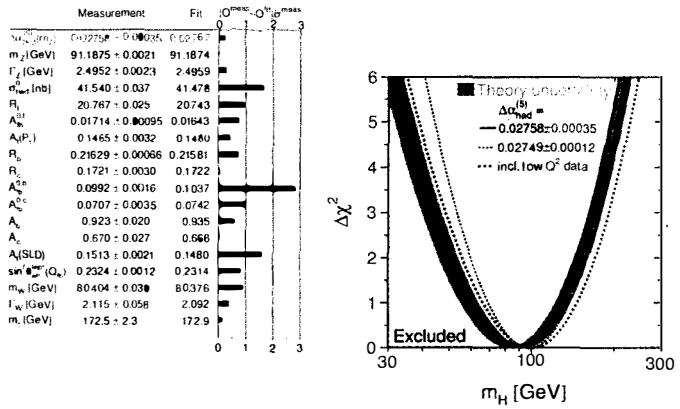

Figure 6: Left: Comparison of the measurements with the SM expectation and the pulls they apply in the global fit. Right: $\delta\chi^2(m_H) = \chi^2_{min}(m_H) - \chi^2_{min}$ of global SM fit as a function of m_H compared to the 95% yellow exclusion zone from LEP and including theoretical uncertainties (band), the effect of different estimates for α_{QED} renormalization at the Z^0 pole and the impact of adding low Q^2 measurements in the fit. The used top and W mass are the updated results for Winter 2006.

References

1. The ALEPH DELPHI L3 OPAL SLD Collaborations, the LEP Electroweak Working Group, the SLD Electroweak and Heavy Flavour Groups [hep-ex/0509008], accepted by Physics Reports and references therein
2. *Physics at LEP2*, eds. G. Altarelli, T. Sjöstrand and F. Zwirner, CERN 96-01, (1996) and references therein.
3. The LEP Collaborations ALEPH, DELPHI, L3, OPAL and the LEP Elctroweak Working Group CERN-PH-EP/2005-051, [hep-ex/0511027] and references therein
4. OPAL Collaboration, G. Abbiendi *et al.*, Phys. Lett. **B609** (2005) 212 [hep-ex/0410034]
5. L3 Collaboration, P. Achard *et al.*, [hep-ex/0603022], to appear in the Eur. Phys. J. **C**
6. M. Grünewald *et al.*, [arXiv:hep-ph/0005309] and references therein.
7. ALEPH Collaboration, S. Schael *et al.*, [hep-ex/0605011], submitted to Eur. Phys. J., **C**,
8. L3 Collaboration, P. Achard *et al.*, Eur. Phys. J. **C45** (2006) 569, [hep-ex/0511049]
9. OPAL Collaboration, G. Abbiendi *et al.*, Eur. Phys. J. **C45** (2006) 307, [hep-ex/0508060]
10. The LEP Energy Working Group, R. Assmann *et al.*, Eur. Phys. J. **C39** (2005) 253
11. T. Sjöstrand and L. Lönnblad, Eur. Phys. J. **C2** (1998) 165
12. T. Sjöstrand and V. A. Khoze Z. Phys. **C62** (1194) 281 and Phys. Rev. Lett. **72** (1994) 28
13. http://lepewwg.web.cern.ch/LEPEWWG/